



Spatio-temporal reconstruction of lahars on the southern slopes of Colima volcano, Mexico – A dendrogeomorphic approach



Oswaldo Franco-Ramos^a, Markus Stoffel^{b,c,*}, Lorenzo Vázquez-Selem^a, Lucia Capra^d

^a Instituto de Geografía, Universidad Nacional Autónoma de México, Ciudad Universitaria, Coyoacán, 04510, México D.F. México

^b Dendrolab.ch, Institute of Geological Sciences, University of Bern, Baltzerstrasse 1 +3, CH-3012 Bern, Switzerland

^c Climatic Change and Climate Impacts, Institute for Environmental Sciences, University of Geneva, 7 route de Drize, CH-1227 Carouge, Switzerland

^d Centro de Geociencias, Universidad Nacional Autónoma de México, Campus Juriquilla, 76230 Querétaro, México

ARTICLE INFO

Article history:

Received 8 July 2013

Accepted 29 September 2013

Available online 11 October 2013

Keywords:

Dendrogeomorphology

Colima volcano

Lahars

Tree rings

Pinus leiophylla

ABSTRACT

Historical records of lahar occurrence and distribution are typically scarce in volcanic environments, even more so if they occur outside of human settlements. In the context of hazard assessment and process understanding, documenting their temporal frequency and drivers of activity might be crucial. On forested volcanoes, lahars may significantly damage trees along their flow paths, and sometimes even eliminate entire forest stands. This study is based on growth disturbances in trees affected by lahars (i) to assess the potential of dendrogeomorphic techniques in lahar research and (ii) to analyze the temporal frequency and spatial patterns of lahars at Montegrande and Arena, two of the most active of the ephemeral streams on the southern sector of Colima volcano. A total of 78 *Pinus leiophylla* live trees were sampled along the ravines, yielding evidence for 20 lahar events after the AD 1913 eruption, adding seven events to the historic records. Although the number of lahars reconstructed with tree-ring records can only be considered as a minimum frequency, the method clearly improves the local lahar chronology. Despite the scarcity of meteorological records at the study sites, the timing of reconstructed lahars points to heavy rainfalls after explosive activity as the main driver of events.

© 2013 Elsevier B.V. All rights reserved.

1. Introduction

Growth anomalies in trees have been used in varying geomorphic and bioclimatic contexts to reconstruct the temporal frequency, spatial distribution or triggers of hydrogeomorphic processes (Alestalo, 1971; Stoffel et al., 2010). Based on the concept of *process-event-response* (Shroder, 1978), trees will record external disturbances induced by the process under investigation in their growth-ring record and thus yield precise chronometric data with at least annual to seasonal resolution (Stoffel and Bollschweiler, 2008). Past work on hydrogeomorphic processes (Stoffel and Wilford, 2012) focused mostly on the temporal frequency, magnitude and spread of (flash) floods (Yanosky and Jarrett, 2002; Ballesteros Cánovas et al., 2011; Ballesteros et al., 2011; Stoffel et al., 2012; Ruiz-Villanueva et al., in press) and debris flows (Bollschweiler et al., 2007, 2008; Stoffel et al., 2008; Procter et al., 2012), but much less so on the occurrence of volcanic lahars (Pearson et al., 2005; Solomina et al., 2008).

Past tree-ring studies in Mexico have shown that a number of subtropical species forms annual growth rings and that these trees are therefore suitable for dendrochronology (Stahle et al., 2000; Villanueva

Díaz et al., 2010). Tree ring research on Mexican volcanoes is above all related to the consequences of eruptions and associated tephra fallout on tree growth. Biondi et al. (2003), for instance, analyzed abrupt suppression in radial growth caused by the tephra fallout of the 1913 Colima eruption. Sheppard et al. (2008) studied suppressed ring widths as well, but also investigated wood anatomical and dendrochemical changes in growth rings associated with tephra fallout of the 1943–1952 eruption of Parícutin volcano. Cruz-Muñoz et al. (2008) observed increased concentrations of P, S, and K in growth rings of trees growing on the slopes of Popocatepetl volcano since 1991. Dendrogeomorphic research in México started with the reconstruction of 20th-century lahars on the NE slope of Popocatepetl volcano (Bollschweiler et al., 2010). The potential of dendrogeomorphology in México was further demonstrated by Stoffel et al. (2011) who reconstructed rockfall activity at a timberline site of dormant Iztaccíhuatl volcano.

Colima is one of the most active volcanoes of Mexico and has almost constantly threatened villages on its slopes as a result of frequent explosive activity since pre-Hispanic times (Bretón-González et al., 2002). Contemporary activity is strongest on the southern flanks of the volcano where several lava and pyroclastic flows as well as lahars have been emplaced during the last few decades (Luhr, 2002; Saucedo et al., 2005). As a consequence of the reactivation of explosive activity in 1991, large volumes of loose pyroclastic material have recharged many of the ravines of Colima volcano, and thus promoted an increase

* Corresponding author at: Dendrolab.ch, Institute of Geological Sciences, University of Bern, Baltzerstrasse 1 + 3, CH-3012 Bern, Switzerland. Tel.: +41 31 631 87 73; fax: +41 31 631 43 41.

E-mail address: markus.stoffel@dendrolab.ch (M. Stoffel).

in the frequency and magnitude of wet season (June–October) lahars (Davila et al., 2007; Capra et al., 2010). Important lahar events have been recorded namely in 1991–92, 1994–95, 2000, 2003, 2007 (Gavilanes Ruiz, 2004), and most recently in 2011, with the latter one being triggered by a hurricane-induced extreme rainfall (Capra et al., in review).

The aims of this study therefore are (i) to document the signatures left by documented lahars in woody vegetation; (ii) to identify older, unknown lahars via the study of growth disturbances (GD) in *Pinus leiophylla* trees; and (iii) to compare the reconstructed lahar time series with data on volcanic activity and instrumental records of rainfall. This study focuses in particular on Montegrande and Arena as these ravines have been proven very susceptible to lahar generation and as lahars in these ravines may potentially affect the town of Queseria (ca. 8611 inhabitants) and San Marcos (ca. 3550 inhabitants).

2. Colima volcano

Colima volcano (19° 30'44.8" N; 103° 37'01.6" W., 3860 masl), also known as Volcán de Fuego, is located in the western sector of the Trans-Mexican Volcanic Belt, in the southern part of the Colima graben system. It formed during the Holocene and represents the youngest volcanic structure of the Colima Volcanic Complex (Saucedo et al., 2010) (Fig. 1). As typical of strato-volcanoes, its chemical composition ranges from andesitic to dacitic. The evolution of Colima volcano includes several partial edifice collapses with associated debris avalanches (Komorowski et al., 1997). Activity in historical times has been diverse in eruptive styles and intensity, and includes three Plinian events (1576, 1818, and 1913) and several Soufrière–Merapi type dome collapse events (Lühr, 2002; Macías et al., 2006; Saucedo et al., 2010; Roverato et al., 2011). One of the most important explosive eruptions

of Colima occurred in 1913, thereby producing voluminous pyroclastic flows and lahars on the southern slopes and considerably modifying the morphology of the crater (Robin et al., 1991; Bretón-González et al., 2002; Saucedo et al., 2010). After a period of relative quiescence, new manifestations occurred in 1961–62, 1963–74, 1975–79, 1981–82, 1985–87, 1991, 1994, 1998–99, 2001 and 2004–05 (Bretón-González et al., 2002; Saucedo et al., 2005; Zobin et al., 2007; Capra et al., 2010).

2.1. Lahars at Colima volcano

Lahars are a very common phenomenon at Colima volcano and include (i) debris flows from sector collapses ($>1 \text{ km}^3$; Capra and Macías, 2002; Cortes et al., 2010), (ii) post-eruptive lahars following the emplacement of pumice flow deposits associated with the AD 1913 Plinian eruption (volume $\sim 5 \times 10^6 \text{ m}^3$, flow distance $\sim 20 \text{ km}$; Saucedo et al., 2010), and (iii) flows induced by extreme hydrometeorological conditions, such as during the AD 1955 Atenuique debris flow that originated from the SE slope of Nevado de Colima, killing 23 people in the homonymous village and emplacing a $3.2 \times 10^6 \text{ m}^3$ deposit (Saucedo et al., 2008).

More frequently, however, lahars are triggered during the rainy season (June–October). These lahars occur in most ravines and may reach distances $\leq 15 \text{ km}$ (Davila et al., 2007; Capra et al., 2010). Sediment sources are more readily available after major eruptive phases, and thus favour the occurrence of more and larger-magnitude lahars as compared to periods with less volcanic activity. Rain-induced lahars are characterized by two main types of flow: (i) debris flow ($>50\%$ vol of sediment) emplacing massive units, with centimetric to decimetric clasts embedded in a sandy matrix; and (ii) more dilute hyperconcentrated flow (20–50% vol in sediment) forming massive, sandy layers.

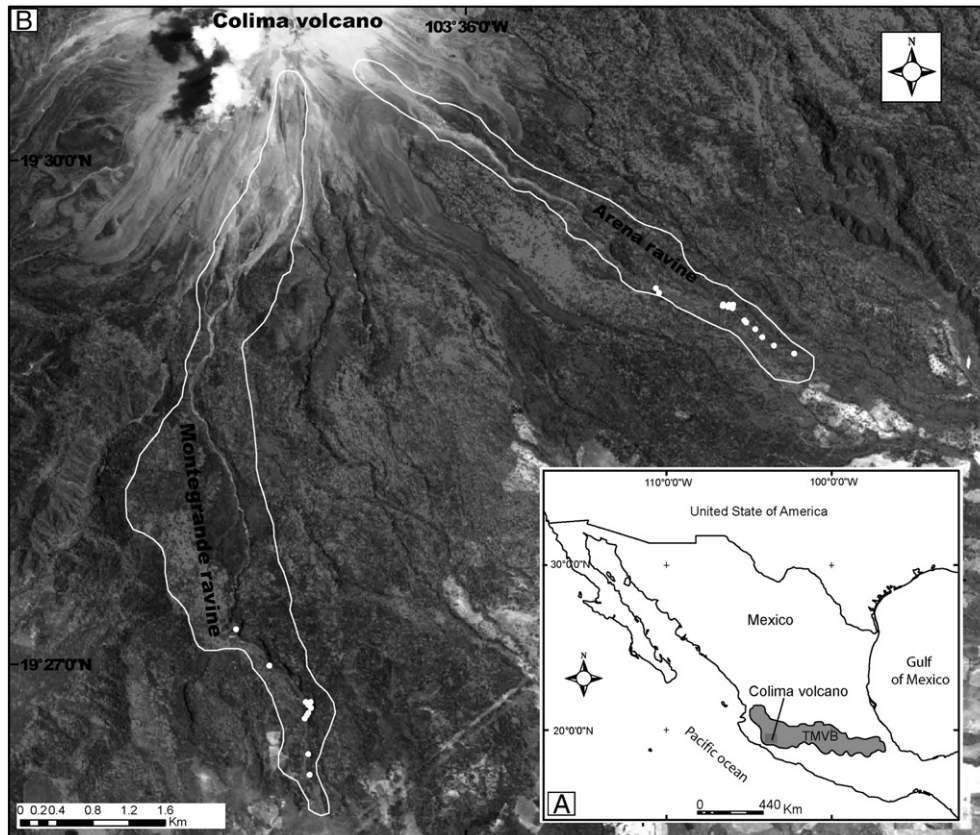


Fig. 1. The study area is located on the southern slope of Colima volcano, in the western part of the Transmexican Volcanic Belt (A). Dendrogeomorphic work in the Montegrande and Arena basins (white lines) have been carried out at altitudes of 1700–1900 masl (white dots) (B).

Past assessments of spatial and temporal patterns of historic lahar activity were repeatedly hampered by the difficulty to recognize different lahar units in the field and to determine their age, especially on sites like Colima where erupted products are homogeneous in composition. At Colima, seismological monitoring has been used to detect major lahars over a period of six years (Davila et al., 2007; Zobin et al., 2009; Capra et al., 2010), but only few data and limited eyewitness reports exist for older activity. Based on the analysis of seismological and rainfall records, no direct correlation seems to exist between rainfall amounts (and intensity) and lahar frequency (Capra et al., 2010). Lahars tend to occur even more frequently during short-lived events with limited rainfall (10–20 mm) early in the rain season and at variable rainfall intensities (20–80 mm h⁻¹). The occurrence of early-season lahars is most likely due to the large amounts of landslide sediments that typically accumulate at the bottom of ravines over the course of the dry and windy season, but also reflective of hydrophobic characteristics of local soils which enhance water runoff and lahar generation even with low rainfall totals. The lahars occurring during this time of the year are typically small and have volumes $0.2 \times 10^6 \text{ m}^3$. In contrast, lahars occur less frequently but with larger volumes (0.3–0.5 × 10⁶ m³) in August–October when more prolonged rainfalls associated with tropical storms release larger amounts of rainfall (up to 100 mm) with more moderate peak intensities (~50 mm h⁻¹) (Capra et al., 2010, in press).

3. Morphology and stratigraphy of Montegrando and Arena ravines

Present-day topography of the SE flanks of Colima volcano is dominated by the overlapping San Marcos (>25 kyr BP) and Tonila (~15 kyr BP) debris avalanche deposits, through which the ravines of Montegrando, Arena-Rosario, El Muerto, Beltran, Los Lobos and Platanera have been cutting over the Holocene (Roverato et al., 2011).

The drainage basin of Montegrando ravine starts at 3600 masl on the S flank of the volcanic cone and has an area of 6.2 km²; average slope angles are 30° in the upper (3600–2700 masl) and 14° in the lower part (2700–1700 masl). The drainage basin of Arena extends from 3400 to 1730 masl on the SE side of the edifice and has an area of 2.3 km²; average slope angles are >31° in the upper (3400–2600 masl) and 15° in the lower part. Recent lava flows have disconnected the Arena drainage basin from the main volcanic edifice (Luhr, 2002), likely resulting in smaller rainfall-derived runoff as compared to the Montegrando basin which is still connected to the edifice and larger in size. The Montegrando and Arena ravines run through the towns of Quesería and San Marcos, respectively, and join the Naranjo River further to the southeast (Fig. 1).

Three main geomorphic units can be recognized inside the ravines (Fig. 2) in the form of terraces. T-1 is a relatively wide, discontinuous high terrace located on older debris avalanche deposits; it is 1–4 m high, a few to several tens of meters wide, with individual stretches up to a few tens of meters long, and a slope angle of up to 8°. The composite stratigraphic section of this terrace consists of scoria and/or pumice flow deposits from the AD 1913 Plinian eruption at its base (Saucedo et al., 2010), overlain by several layers of debris-flow deposits of the same eruptive phase. Deposits are usually massive, heterolithic in composition, with rounded to subrounded clasts embedded in abundant fine-sand matrix. T-1 terraces are mostly stable and covered with dense forest (Fig. 3).

The second unit (T-2) consists of terraces and fills emplaced inside channels eroded into unit T-1. Channels of T-2 are no longer active, with the exception of a few incipient channels. The unit is sloping gently in the flow direction (5° on average), of smaller dimension than T-1 and with irregular shapes. T-2 consists of debris-flow deposits with thicknesses <1 m, heterolithic centimetric to decimetric size clasts embedded in a sandy matrix, intercalated with thinner hyperconcentrated flow deposits consisting of massive sandy units. T-2 is younger than T-1, only has a thin soil layer (a few cm deep), and an open forest with young trees. Buried, tilted and impacted live trees are common in the laharic deposits of T-2, and surfaces tend to be unstable (Fig. 3).

The third unit consists of recent deposits associated to lahars along the active flow channel at Montegrando and Arena. Deposits are <4 m thick and consist of alternations of debris-flow and hyperconcentrated flow deposits. Debris-flow deposits are common along the ravines and contain block sizes <3 m in diameter embedded in a sandy matrix. In the most stable channel segments an incipient vegetation cover can be found, characterized by centimetric herbaceous plants (Fig. 3).

Debris flows at Colima volcano are characterized by turbulent, block-rich fronts, with clasts >1 m in diameter, followed by a well-developed body with laminar flow behavior that has been reported to flow continuously from the upper portion of the ravine to down valley locations for >30–40 min or >1–2 h during prolonged tropical storm events. Such debris flows are also responsible for the largest damage to infrastructures such as in 1999 and 2007 when electricity pylons at the base of Montegrando ravine were destroyed completely.

Trees growing in the study area consist of a pine-oak forest. *P. leiophylla* Schiede ex. Schltdl. et Cham., is the most abundant conifer species in Montegrando and Arena. This species is widely distributed from the Sierra Madre Occidental and the Transmexican Volcanic Belt to some sectors of the Sierra Madre del Sur, at altitudes ranging from 1500 to 3300 masl (Farjon and Styles, 1997). In Mexico, 20 species of

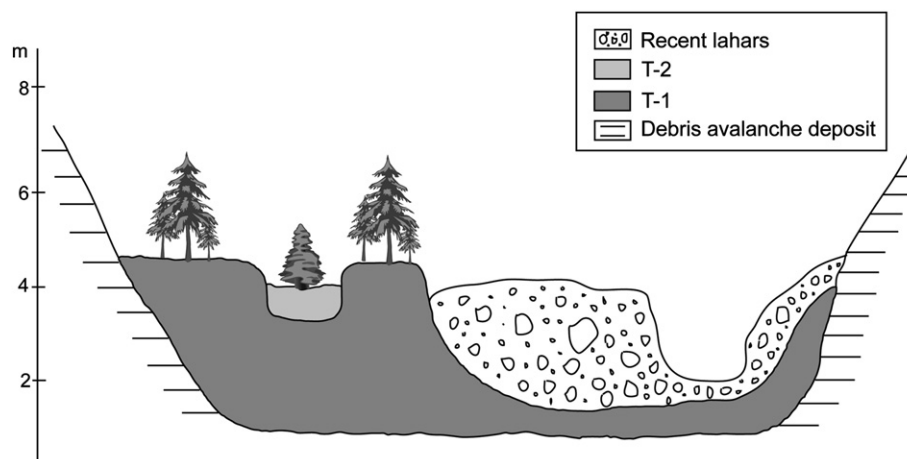


Fig. 2. Schematic profile of debris flows and terraces in the Montegrando and Arena ravines, formed by lahars after the 1913 Plinian eruption of Colima volcano. Terrace T-1 consists of deposits of the 1913 eruption, T-2 is of younger age.

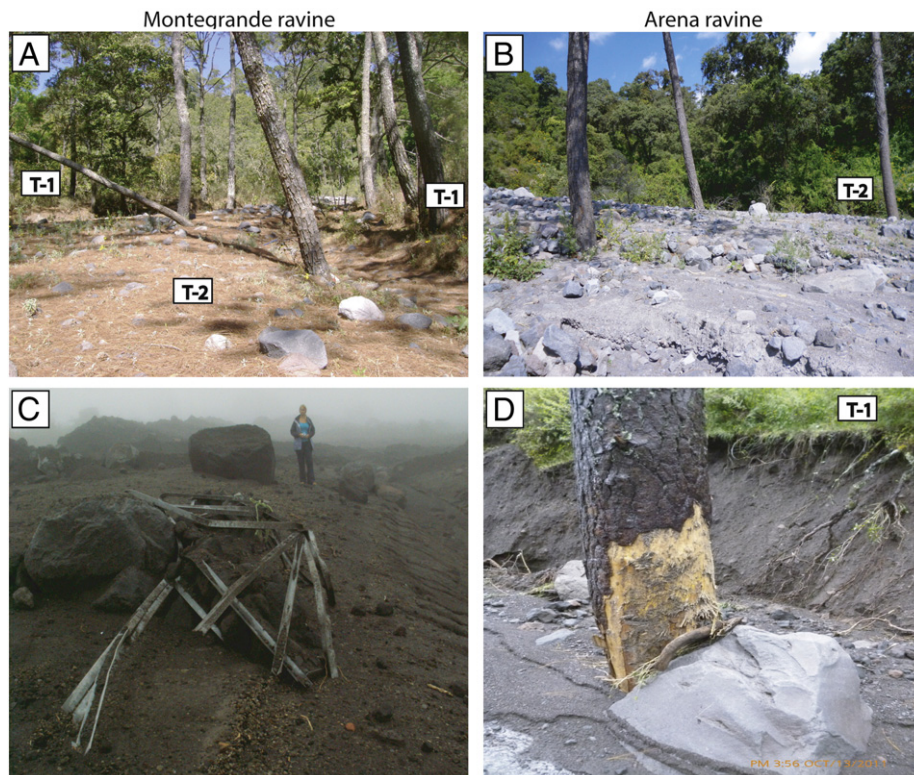


Fig. 3. Illustrations of terraces and recent deposits in the Montegrande and Arena ravines. Trees growing next to the present-day channel and on the terraces show multiple signs of damage in the form of (A) tilted and/or (B) buried stems as well as through the presence of (D) injuries. (C) Damage caused to the powerline by a lahar event in the Montegrande ravine.

Pinus have been used in tree-ring research (Stahle et al., 2000; Villanueva Díaz et al., 2010), but these did not include *P. leiophylla*. Sheppard et al. (2008) stated in their work that they have used *P. leiophylla* along with other pine species to identify dendrochemical signatures of the Parícutin eruption, but did not provide any information about the potential of the species.

4. Materials and methods

Lahar reconstruction at Montegrande and Arena was performed at elevations of 1700 and 1900 masl (Figs. 1 and 3) and in areas where field evidence pointed to frequent lahar activity (mostly from passing lahars, but also in the form of deposition) and associated damage in trees. Following geomorphic mapping of the two sectors at a scale of 1:1000, we systematically sampled 78 living *P. leiophylla* trees showing obvious signs of burial (by 0.5 to 2 m of debris), or tilting and injuries by past lahars. Trees without signs of lahar disturbance were not sampled, except for 15 trees located on terrace T-1 which were used to build a reference chronology. At Montegrande, 56 trees were sampled with 115 increment cores, 3 cross-sections and 2 wedges (120 samples). At Arena, samples were taken from 22 trees and included 44 increment cores, 2 cross-sections and 2 wedges (48 samples; Table 1). Sampling followed the standard procedures as described by Stoffel and Bollschweiler (2008) and included the extraction of at least two

Table 1
Type and number of dendrogeomorphic samples of 78 *Pinus leiophylla* analyzed in the Montegrande and Arena ravines.

	Montegrande	Arena	Total
Increment cores	115	44	159
Cross sections	3	2	5
Wedges	2	2	4
Total	120	48	168

increment cores per tree as well as the gathering of tree-specific data (tree height, diameter at breast height, sampling height, microtopography and inferred processes, visible growth defects, distance of trees with respect to the main channel; also see Stoffel et al., 2005 and 2013 for details).

Sample analyses followed the procedures described by Stoffel and Corona (in press). These included ring-width measurements using a Leica microscope connected to a LINTAB measuring device and TSAP software (Time Series Analysis and Presentation; Rinntech, 2012). Growth curves of disturbed trees were cross-dated with a local reference chronology – representing undisturbed growth conditions – so as to locate potentially missing rings in the disturbed series and to distinguish climatic from geomorphic signals in the growth ring series. Disturbances observed in individual trees were then weighted depending on the intensity of their response to the impact (Kogelnig-Mayer et al., 2011) and illustrated in a GIS to see the spatial distribution of trees affected by individual lahar events. Depending on the number of trees reacting to a lahar, we also distinguish between certain and possible years, thereby differentiating events dated with a large number of growth disturbances (GD) and high confidence from those dated with fewer trees exhibiting GD and thus lesser confidence. The final list of years with lahar activity was then compared with information from historical archives, eruptive chronologies and precipitation data from the closest meteorological station in the region (San Marcos; CLICOM, 2006), located ~7 km to the SE of Arena ravine study site at an altitude of 1200 masl.

5. Results

5.1. Montegrande ravine

The mean age of trees at Montegrande is 79 yr (SD = 9.2 yr), thus suggesting widespread colonization and fairly stable conditions after the AD 1913 Plinian eruption. Along the same line of thought, the oldest

trees can generally be found on the higher parts of T-1 and farthest away from the present-day ephemeral channel. The oldest tree sampled at Montegrade ravine colonized terrace T-1 in AD 1920, whereas the youngest *P. leiophylla* reached sampling height in 1978 (Fig. 4).

Analysis of the 120 tree-ring records from Montegrade ravine exhibits 158 GD related to past lahar activity. Growth suppression following stem burial or root exposure was observed most frequently (56%), followed by chaotic callus tissue bordering wounds (17%) and impact scars (9%), with the latter representing the most intense dendrogeomorphic growth anomaly. Other effects were observed less frequently: growth release due to elimination of neighboring trees (7%), or eccentric growth (6%) and development of compression wood (5%) due to tree tilting (Table 2).

Based on the analysis of GD in space and time, a total of 15 years with lahar activity could be reconstructed for the Montegrade ravine for the past ~40 yr. Eleven of these lahars left a large number of GD in the tree-ring series and could therefore be reconstructed with high certainty. These certain events occurred in 1969, 1976, 1982, 1984, 1987, 1991, 1994, 1998, 2004, 2008, and 2011. In 4 cases, event reconstruction was based on a more limited number of responding trees and the occurrence of lahars should be considered probable in 2001, 2005, 2007, and 2009 (Fig. 4).

The most important lahar in terms of GD intensity and number of affected trees occurred in 1994 and resulted in one-third of all GD recorded in the selected trees. Stem burial and related growth suppression were observed in 25 trees of terrace T-2 and in 17 trees of T-1, and 5 trees located next to the active channel showed impact scars. The lahar of 2004 was important as well in terms of lateral spread and surfaces affected, but were clearly smaller and restricted to the lower terrace T-2 and next to active channels (Fig. 5).

5.2. Arena ravine

The mean age of trees at Arena ravine is 76 yr (SD = 16 yr). The oldest tree is dated to AD 1913 and the youngest sample reached sampling height in 1983. Similar to the situation at Montegrade, older trees are

Table 2
Growth disturbances associated with lahar activity at Montegrade and Arena ravines.

	Montegrade		Arena		Total	
	#	%	#	%	#	%
Compression wood	8	5	5	7	13	6
Injury	14	9	10	14	24	10
Callus tissue	27	17	6	8	33	14
Growth suppression	89	56	35	47	124	53
Growth release	11	7	15	20	26	11
Eccentric growth	9	6	3	4	12	5
Total	158	100	74	100	232	100

typically located on terrace T-1 and apparently colonized the newly created surfaces immediately after the emplacement of the pyroclastic flow and lahar of deposits of the 1913 eruption (Fig. 4).

Analysis of the 48 tree-ring records from Arena ravine exhibit 74 GD related to past lahar activity. Again, growth reactions to disturbance by lahars are typically in the form of abrupt growth suppression (47%), impact scars (14%) and callus tissue (8%). At Arena, the removal of neighboring vegetation seems to be more crucial than at Montegrade, with frequent observation of growth releases (20%) in the tree-ring records of survivor trees (Table 2).

A total of 11 lahars could be reconstructed for the Arena ravine over the past ~30 yr. Eight of the events (1979, 1991, 1994, 1996, 1999, 2005, 2006, and 2011) can be reconstructed with high certainty whereas 3 events (AD 1986, 2004 and 2009) were identified in a somewhat smaller number of trees (Fig. 4). The geomorphic map shows trees buried and injured by lahars in 1994 (19% of all GD) and 2005 (11%). All of the reacting trees at Arena are in fact located on the low terrace (T-2) and next to the main channel (Fig. 6), and reactions are clearly missing in trees growing on T-1.

6. Discussion

This contribution focuses on a dendrogeomorphic reconstruction of past lahar activity in the Montegrade and Arena ravines located on

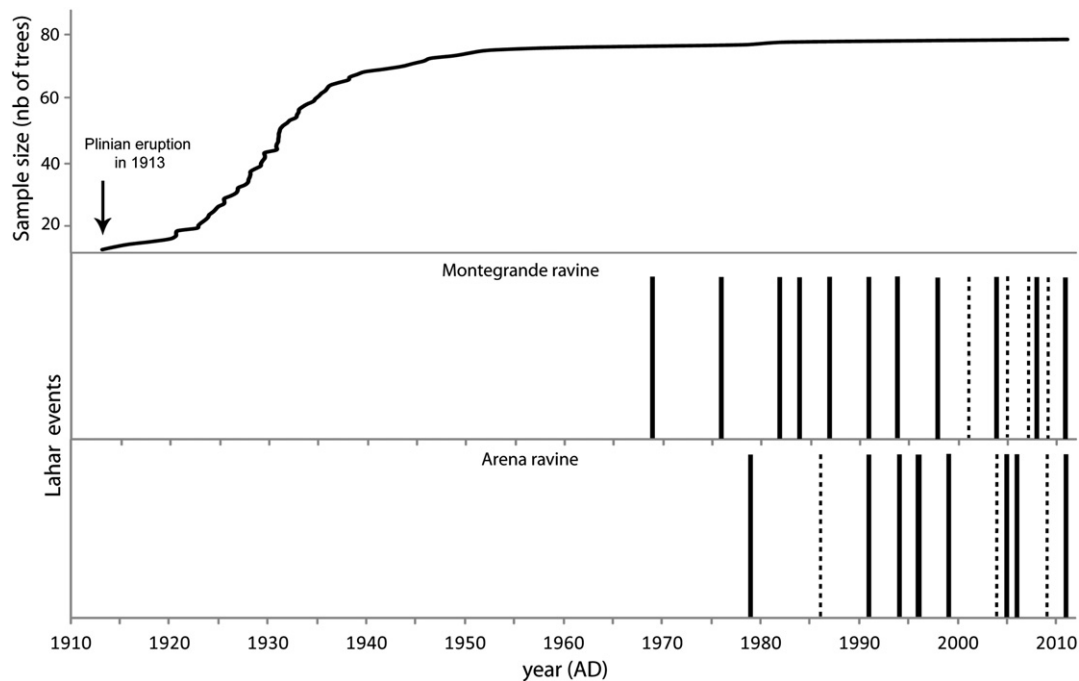


Fig. 4. Number of live trees sampled and lahar events reconstructed with dendrogeomorphic techniques at Montegrade ($n = 15$) and Arena ($n = 11$). Six events were likely triggered by the same rainfall event in both ravines. Bold lines indicate lahars with growth disturbances in a large number of trees. For lahars presented with dashed lines, the number of responding trees was more limited and events should be considered probable. For details see text.

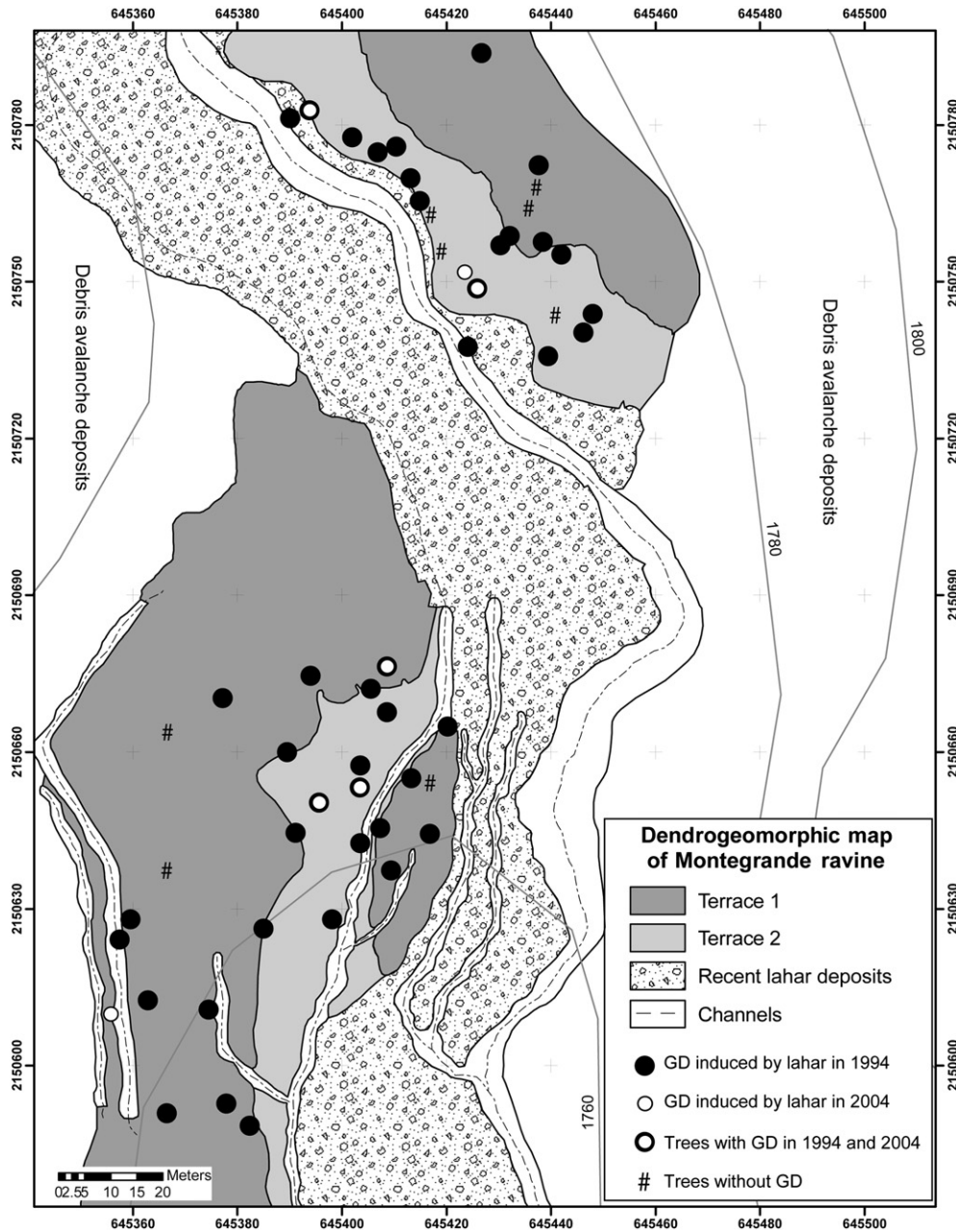


Fig. 5. Geomorph map of Montegrande ravine and location of trees affected by the 1994 and 2004 lahars.

the SE flanks of Colima volcano, México. Although *P. leiophylla* produces both false and missing rings in some years, it clearly forms annual rings. The growth series could be crossdated and proved to be very suitable for dendrochronological purposes. The study was successful in reconstructing lahar chronologies for both sites and covering several decades, and thus confirms the considerable potential of an increasing number of Mexican tree species for dendrogeomorphic research (Bollschweiler et al., 2010; Stoffel et al., 2011).

The mean age of the trees sampled in both ravines is 78 yr, and a vast majority of individuals (80%) reached sampling height (i.e. 20–80 cm above ground) between 1920 and 1940, thus pointing to germination ages somewhere in the late 1910s to mid-1930s (Bollschweiler et al., 2008; Koch, 2009). The oldest tree of this study germinated in 1913; because it grows on a well-protected site above T-1, the tree in question apparently is the only local survivor of the first generation established after the 1913 Plinian eruption (Figs. 5 and 6). As a consequence of

the very regular occurrence of lahars in the ravines and due to logging by the local population, trees established just after the 1913 eruption have proven scarce today.

Almost half of the 232 GD identified in the tree-ring records of Montegrande and Arena ravines are in the form of abrupt growth suppression and thus point to the frequent occurrence of stem burial and root exposure processes. Observations in the field confirm frequent changes in channel bed locations, avulsions and recent lahar infills by debris and hyperconcentrated flows within the current lahar channel as well as on terrace T-2.

Channel incision can be caused by debris flows or hyperconcentrated flows, and an attribution of causative processes will be virtually impossible in this case. Massive stem burial and the infliction of elongated scars (with related callus tissue) have been demonstrated to be rather scarce in trees affected by hyperconcentrated flows and debris floods (Bollschweiler et al., 2007; Mayer et al., 2010; Stoffel and Corona, in press), even more so in trees with thick bark structures as

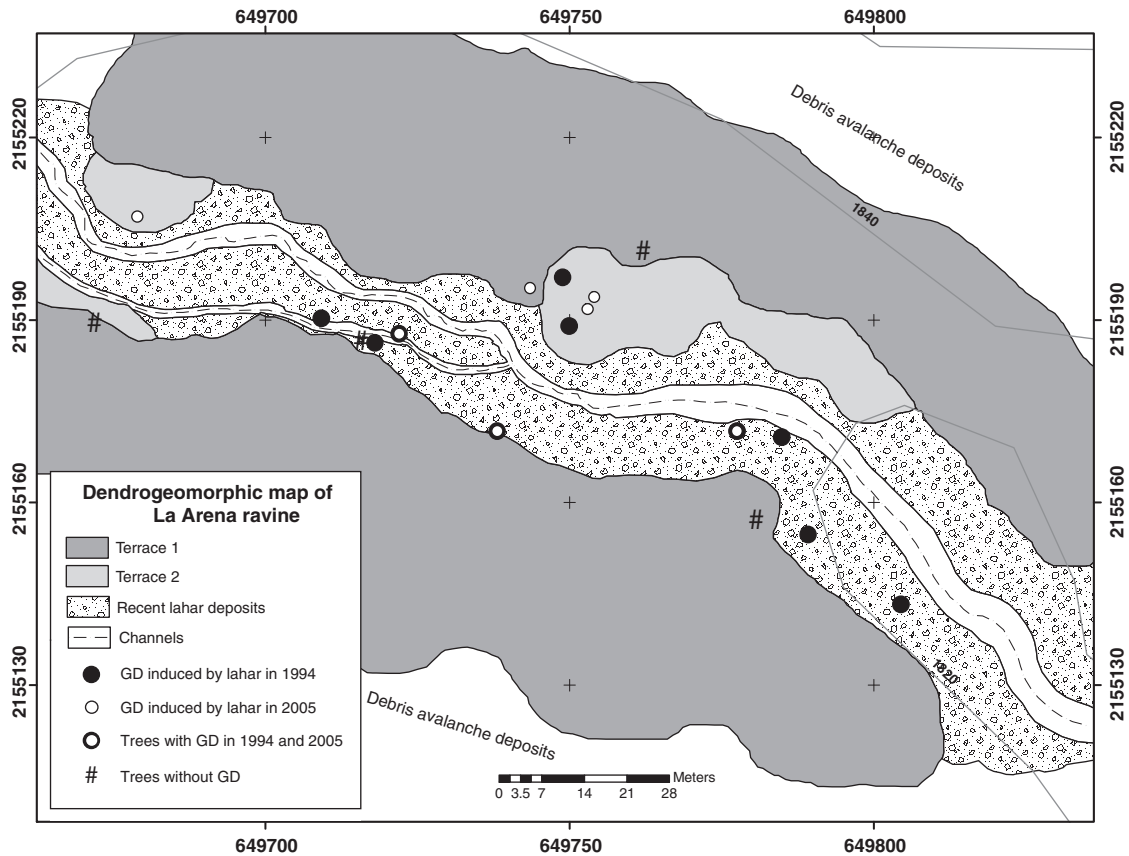


Fig. 6. Geomorphologic map of Arena ravine and location of trees affected by the 1994 and 2005 lahars.

is the case of *Pinus* sp. (Stoffel and Perret, 2006; Šilhán et al., in press). We can thus assume that much of the observed damage in the trees sampled at Montegrande and Arena ravines has been induced by metric blocks transported in debris flows. In the same line of thoughts, we may thus speculate that a majority of the reconstructed events would be larger lahars ($0.3\text{--}0.5 \times 10^6 \text{ m}^3$) that would have been triggered by more intense hydro-meteorological situations that are typical during tropical storms occurring toward the end of the wet season. In those cases, Colima volcano is typically affected by long-lasting rains, and lahars are typically registered in all main ravines. In the case of reconstructed lahars causing a limited number of mostly weak GD in trees, one could think of more isolated, short-lived, early season rainfalls forming smaller debris flows ($<0.2 \times 10^6 \text{ m}^3$; Capra et al., in review) or of more dilute flows transporting fewer big blocks.

Table 3 provides a summary of the lahar reconstruction based on tree rings along with the pre-existing historic (post-1913) lahar record, years of eruptive activity and rainfall data. The historic record of lahars does not specify the number of lahar occurrences in the same year, except for the most recent period (2004–2011) for which the record is based on seismic signals. During this period, at least 5 lahars or sediment laden flows were recorded every year.

Events recorded simultaneously in the Montegrande and Arena ravines and showing a large number of heavily impacted trees (i.e. strong GD in the tree-ring record) could therefore be attributed to extreme hydrometeorological events. By contrast, events recorded in only one of the ravines and showing a more limited level of disturbance in trees – both in the number and intensity of GD – could thus be indicative of moderate rainfalls or more dilute flows.

Several limitations, however, exist to demonstrate this link between damage to trees and rainfall amounts (intensities). First of all, lahars recorded in *P. leiophylla* trees are dated to the year, rendering a clear attribution of damage to a specific rainfall quite difficult. In addition,

the rainfall data from San Marcos certainly is valuable to capture tropical hurricanes, but will likely underestimate or even miss localized thunderstorm cells triggering lahars in single ravines. As a consequence, Table 3 only aims at presenting possible connections between lahars reconstructed from the tree-ring records and specific hydrometeorological events registered at San Marcos, without assuming to calendar-date the time series of 20 lahars for the Montegrande and Arena ravines. In addition to providing the largest record of recorded liquid precipitation for each of the years with reconstructed lahar activity, Table 3 also presents possible connection of lahars with volcanic activity at Colima volcano and the emplacement of block-and-ash flow deposits that may have fed main ravines with loose material. Fourteen out of the 20 reconstructed lahars (70%) coincide with years of reported volcanic activity at Colima (Bretón-González et al., 2002; Saucedo et al., 2005), namely 1969, 1976, 1979, 1982, 1984, 1986, 1987, 1991, 1994, 1998, 1999, 2001, 2004, and 2005 (Table 3). Our data thus suggest that the syn- or post-eruptive occurrence of lahars, documented at Colima volcano since 1913, must have occurred during earlier major eruptive phases as well. Interestingly, before 1988 all the lahars occurred only in one of the two ravines (either Montegrande or Arena) and they left fewer and less intense GD to trees. The observation of changes in the intensity and number of GD are consistent between the ravines and cannot be attributed to methodological biases because the age and overall number of trees available for analysis remain virtually constant over the past 30–40 years. We can thus speculate that the pre-1988 lahars recorded in the tree-ring series might have occurred during rainfalls of shorter duration but higher peak intensity that is common for the early rainy season.

The lahar activity of 1991, 1994, 2004, 2005, 2009, and 2011, by contrast, is detected in both ravines, and events are associated with more intense and larger numbers of GD. One might thus assume that these lahars were triggered by more intense hydrometeorological

Table 3

Lahar chronology inferred from tree-ring records at Montegrando and Arena ravines, lahars reported inside the main active ravines on the southern slopes at Colima volcano and rainfall data (extreme events) recorded at San Marcos meteorological station, located ~7 km from the Arena sampling site (CLICOM, 2006). Information on hurricanes and tropical storm were gathered from the Historical Hurricane Track NOAA database (<http://csc.noaa.gov/hurricanes/#>).

Lahar events identified by tree-ring analysis			Lahar events reported on main active ravines on the southern slopes of Colima volcano								Maximum rainfall data		
Year AD	Montegrando	Arena	L	Z	SC	SA	M	C	A	References	Amount (mm)	Accumulation (days)	Hurricanes & tropical storms
1913-16	**Laharic terrace (T-1)	**Laharic terrace (T-1)	◆	X		◆	X	X	◆	Saucedo et al., 2010; Gavilanes Ruiz., 2004	–	–	–
*1969	X									–	132	4	–
*1976	X		X					X	X	Gavilanes Ruiz., 2004	167	2	–
*1979		X								–	90	2	“ANDRES”
*1982	X							X		Gavilanes Ruiz., 2004	152	1	–
*1984	X									–	132	3	–
*1986		X								–	101	3	–
*1987	X									–	172	2	–
1988	No growth disturbances							X	X	Gavilanes Ruiz., 2004	106	2	–
*1991	X	X			X					Rodriguez-Elizarrarás et al., 1991	65	2	–
1992	No growth disturbances						X			Gavilanes Ruiz., 2004	203	2	–
*1994	X	X			X	X			X	Saucedo et al., 2005	104	2	–
1996		X								–	146	3	“HERNAN”
*1998	X				X					Gavilanes (personal com.)	110	2	–
*1999		X					◆			Davila et al., 2007	198	1	“GREG”
2000	No growth disturbances		X	◆	X					Gavilanes Ruiz., 2004	151	3	“NORMAN”
*2001	X									–	98	3	–
2003	No growth disturbances						◆	◆		Varley (personal com.)	122	2	–
*2004	X	X	>5				>5	X		Davila et al., 2007	121	2	–
*2005	X	X	>5				>5	X		Davila et al., 2007	89	3	“DORA”
2006		X	>5				>5	X		Davila et al., 2007	150	3	“NORMAN”
2007	X		>5				>5	1		Capra et al., 2010	83	3	–
2008	X		>5				>5	2		Capra et al., 2010	110	3	“ODILE”
2009	X	X	>5				>5	2		Capra et al., in press	115	5	–
2010	No growth disturbances		3				>5	3		Capra et al., in press	>200	~4	–
2011	X	X	>5				>5	2		Capra et al., in press	>300	1	“JOVA”

* Volcanic activity reported. ** By tree age calibrated.

>5 = Multiples events, but based only on the seismic record it is not clear if all where lahars or only sediment laden streamflow.

◆ = Damages to infrastructure and animals; L = La Lumbre; Z = El Zarco; SC = Cordoban; SA = San Antonio; M = Montegrando; C = Cafecito; A = Arena; X = lahar event.

events with prolonged rainfall. It is noteworthy that the lahars of 1991, 1994, 2004, and 2005 occurred during years with eruptive activity of Colima volcano, and may thus have had larger sources of loose sediments from fresh pyroclastic flow deposits. The 2009 and 2011 lahars, in contrast, took place during an inter-eruptive phase, but were, in the case of the 2011 lahar, triggered by the Jova hurricane with >300 mm 24 h⁻¹ (Capra et al., in review). The lahars of 1996 are another fine example of hurricane-induced mass wasting (“Hernan” hurricane; NOAA, 2013).

Subsequent to the 1913 Plinian eruptive episode, a total of 25 lahar events were documented either with tree rings (20 events), historical record (18), or in both sources (13). Seven events are documented only in the tree-ring series (1969, 1979, 1984, 1986, 1987, 1996, and 2001) and coincide with years of reported eruptive activity, except for 1996. In this sense, the reconstruction presented in this paper forms a clear improvement of the local lahar chronology at Colima volcano. The fact that five events (1988, 1992, 2000, 2003, and 2010) could not be identified in the tree-ring record is likely due to insufficient tree sampling or the fact that very liquid and/or small events may not damage trees.

7. Conclusions

Lahar activity in Montegrando and Arena ravines was reconstructed using the number and intensity of GD recorded in the tree-ring series of impacted *P. leiophylla*. The approach presented in this paper has proven useful for the reconstruction of event frequencies covering several decades of the past and allowed adding seven events to the historic lahar chronology. At the same time, however, the reconstruction yielded somewhat more limited information on event magnitudes and failed to provide evidence on five reported lahars.

We assume that the volume of lahars and channel geometry (i.e. cross-sectional area) will determine the spread of the flow within the channel and on the terraces and therefore determine the number and the intensity of damage in trees. Despite these limitations, *P. leiophylla* has been proven to be a valuable dendrogeomorphic recorder of post-eruptive processes on Mexican volcanoes, and we therefore call for more dendrogeomorphic research at Colima and comparable environments and for an extension of existing studies with other tree species, including subtropical broadleaved trees.

Acknowledgments

The authors kindly acknowledge Carla Torres Beltran, J.C. Gavilanes, Sergio Salinas, Nick Varley, and various MSc students of Universidad de Colima for their support and advice during fieldwork. They are also grateful to Alfredo Rodríguez Manjarrez and Michelle Schneuwly-Bollschweiler for technical support during sample preparation and laboratory analyses. Special thanks also go to the reviewers for insightful comments. Funding was provided by UNAM-PAPIIT project IN105213.

References

- Alestalo, J., 1971. Dendrochronological interpretation of geomorphic processes. *Fennia* 105, 1–139.
- Ballesteros Cánovas, J.A., Eguibar, M., Bodoque, J.M., Díez-Herrero, A., Stoffel, M., Gutiérrez-Pérez, I., 2011. Estimating flash flood discharge in an ungauged mountain catchment with 2D hydraulic models and dendrogeomorphic palaeostage indicators. *Hydrol. Process.* 25, 970–979.
- Ballesteros, J.A., Bodoque, J.M., Díez-Herrero, A., Sanchez-Silva, M., Stoffel, M., 2011. Calibration of floodplain roughness and estimation of flood discharge base on tree-ring evidence and hydraulic modeling. *J. Hydrol.* 403 (103), 115.
- Biondi, F., Galindo, I., Gavilanes, J.C., Elizalde, A., 2003. Tree growth response to the 1913 eruption of Volcan de Fuego de Colima, Mexico. *Quat. Res.* 59, 293–299.

- Bollschweiler, M., Stoffel, M., Ehmsich, M., Monbaron, M., 2007. Reconstructing spatio-temporal patterns of debris flow activity using dendrogeomorphological methods. *Geomorphology* 84 (4), 337–351.
- Bollschweiler, M., Stoffel, M., Scheuwy, D., 2008. Dynamics in debris-flow activity on a forested cone—a case study using different dendroecological approaches. *Catena* 72, 67–78.
- Bollschweiler, M., Stoffel, M., Vázquez-Selem, L., Palacios, D., 2010. Tree-ring reconstruction of past lahar activity at Popocatepetl volcano, México. *The Holocene* 20 (2), 265–274.
- Bretón-González, M., Ramírez, J.J., Navarro, C., 2002. Summary of the historical eruptive activity of Volcán De Colima, Mexico 1519–2000. *J. Volcanol. Geotherm. Res.* 117, 21–46.
- Capra, L., Macías, J.L., 2002. The cohesive Naranjo debris flow deposit (10 km³): a dam breakout flow derived from the pleistocene debris-avalanche deposit of Nevado de Colima volcano (Mexico). *J. Volcanol. Geotherm. Res.* 117, 213–235.
- Capra, L., Borselli, L., Varley, N., Gavilanes-Ruiz, J.C., Norini, G., Sarocchi, D., Caballero, L., Cortes, A., 2010. Rainfall-triggered lahars at Volcán de Colima, Mexico: surface hydro-repellency as initiation process. *J. Volcanol. Geotherm. Res.* 189, 105–117.
- Capra, L., Roverato, M., Gavilanes-Ruiz, J.C., Gropelli, G., Arambula, R., Sulpizio, R., Reyes Dávila, G.A., Borselli, R., Sarocchi, D., Lube, G., Cronin, S., Rodríguez, L.A., 2013. Hurricane-triggered lahars at Volcán de Colima, western Mexico: evidences of flow dynamics from monitoring and field survey. *Earth Surf. Process. Land.* (in review).
- Capra, L., Gavilanes-Ruiz, J.C., Varley, N., Borselli, L., 2013. Origin, behavior and hazard of rain-triggered lahars at Volcán de Colima. In: Varley, N., Komorowski, J.C. (Eds.), *Volcán de Colima: managing the threat*. Springer (in press).
- CLICOM, 2006. Mexico Climatological Station Network Data. Servicio Meteorológico Nacional (SMN), Base de datos (2006).
- Cortes, A., Macías, J.L., Capra, L.L., Garduño-Monroy, V.H., 2010. Sector collapse of the SW flank of Volcán de Colima, México. The 3600 yr BP La Lumbre-Los Ganchos debris avalanche and associated debris flows. *J. Volcanol. Geotherm. Res.* 189 (1–4), 52–66.
- Cruz-Muñoz, A.R., Rodríguez-Fernández, L., Calva-Vázquez, G., Ruvalcaba-Sil, J.L., 2008. Effects due to Popocatepetl volcano eruptions on the elemental concentrations in tree growth rings. *X-Ray Spectrom.* 37, 163–168.
- Dávila, G.A., Capra, L., Gavilanes-Ruiz, J.C., Varley, N., Norini, G., Gómez Vázquez, A., 2007. Recent lahars at Volcan de Colima (Mexico): drainage variation and spectral classification. *J. Volcanol. Geotherm. Res.* 165, 127–141.
- Farjon, A., Styles, B.T., 1997. *Pinus* (Pinaceae). *Flora Neotropica Monograph* 75. The New York Botanical Garden, New York, NY pp. 291.
- Gavilanes Ruiz, J.C., 2004. Simulación de escenarios eruptivos del volcán de Colima y aportaciones al plan de contingencias del estado de Colima. Tesis de Maestría Facultad de Filosofía y Letras, UNAM (123 pp.).
- Koch, J., 2009. Improving age estimates for late Holocene glacial landforms using dendrochronology – some examples from Garibaldi Provincial Park, British Columbia. *Quat. Geochronol.* 4, 130–139.
- Kogelnig-Mayer, B., Stoffel, M., Schneuwly-Bollschweiler, M., Hübl, J., Rudolf-Miklau, F., 2011. Possibilities and limitations of dendrogeomorphic time-series reconstructions on site influenced by debris flows and frequent snow avalanche activity. *Arctic Antarct. Alpine Res.* 43 (4), 649–658.
- Komorowski, J.C., Navarro, C., Cortes, A., Saucedo, R., Gavilanes, J.C., Siebe, C., Espíndola, J.M., Rodríguez-Elizarrarás, S.R., 1997. The Colima Volcanic Complex. *Fiel guide #3. 'IAVCEI, General Assembly'*. Puerto Vallarta, Mexico.
- Luhr, J., 2002. Petrology and geochemistry of the 1991 and 1998–1999 lava flows from Volcan de Colima, Mexico: implications for the end of the current eruptive cycle. *J. Volcanol. Geotherm. Res.* 117, 169–194.
- Macías, J.L., Saucedo, R., Gavilanes, J.C., Varley, N., Velasco, García S., Bursik, M.L., Vargas, Gutiérrez V., Cortes, A., 2006. Flujos piroclásticos asociados a la actividad explosiva del volcán de Colima y perspectivas futuras. *GEOS* 25, 340–351.
- Mayer, B., Stoffel, M., Bollschweiler, M., Hübl, J., Rudolf-Miklau, F., 2010. Frequency and spread of debris floods on fans: a dendrogeomorphic case study from a dolomite catchment in the Austrian Alps. *Geomorphology* 118, 199–206.
- NOAA, 2013. Historical Hurricane Track NOAA database. accesses 2013 <http://csc.noaa.gov/hurricanes/#>.
- Pearson, C., Manning, S.W., Coleman, M., Jarvis, K., 2005. Can tree-ring chemistry reveal absolute dates for past volcanic eruptions? *J. Archaeol. Sci.* 32, 1265–1274.
- Procter, E., Stoffel, M., Bollschweiler, M., Neumann, M., 2012. Exploring debris-flow history and process dynamics using an integrative approach on a dolomitic cone in western Austria. *Earth Surf. Process. Land.* 37, 913–922.
- Rinntech, 2012. LINTAB-Precision Ring by Ring. <http://www.rinntech.com/Products/Lintab.htm> (accessed May 2012).
- Robin, C., Camus, G., Gourgaud, A., 1991. Eruptive and magmatic cycles at Fuego de Colima volcano (Mexico). *J. Volcanol. Geotherm. Res.* 45, 209–225.
- Rodríguez-Elizarrarás, S., Siebe, C., Komorowski, J.C., Espíndola, J.M., Saucedo, R., 1991. Field observations of pristine block-and-ash-flows deposits emplaced April 16–17, 1991 at Volcán de Colima, Mexico. *J. Volcanol. Geotherm. Res.* 48, 399–412.
- Roverato, M., Capra, L., Sulpizio, R., Norini, G., 2011. Stratigraphic reconstruction of two debris avalanche deposits at Colima Volcano (Mexico): insights into pre-failure conditions and climate influence. *J. Volcanol. Geotherm. Res.* 207, 33–46.
- Ruiz-Villanueva, V., Díez-Herrero, A., Bodoque, J.M., Ballesteros, J.A., Stoffel, M., 2013. Characterization of flash floods in small ungauged mountain basins of central Spain using an integrated approach. *Catena* 110, 32–43.
- Saucedo, R., Macías, J.L., Sheridan, M.F., Bursik, M.L., Komorowski, J.C., 2005. Modeling of pyroclastic flow of Colima Volcano, Mexico: implications for hazard assessment. *J. Volcanol. Geotherm. Res.* 139, 103–115.
- Saucedo, R., Macías, J.L., Sarocchi, D., Bursik, M.L., Rupp, B., 2008. The rain-triggered Atenquique volcanoclastic debris flow of October 16, 1955 at Nevado de Colima Volcano, Mexico. *J. Volcanol. Geotherm. Res.* 132 (1–2), 69–83.
- Saucedo, R., Macías, J.L., Arce, J.L., Komorowski, J.C., Gardner, J.E., Valdez-Moreno, G., 2010. Eyewitness, stratigraphy, chemistry, and eruptive dynamics of the 1913 Plinian eruption of Volcán de Colima, México. *J. Volcanol. Geotherm. Res.* 191 (3–4), 149–166.
- Sheppard, P.R., Ort, M.H., Anderson, K.C., Elson, M.D., Vázquez-Selem, L., Clemens, A.W., Little, N.C., Speakman, R.J., 2008. Multiple dendrochronological signals indicate the eruption of Parícutin volcano, Michoacán, Mexico. *Tree-Ring Res.* 64 (2), 97–108.
- Shroder, J., 1978. Dendrogeomorphological analysis of mass movement on Table Cliffs Plateau, Utah. *Quat. Res.* 9, 168–185.
- Šilhán, K., Pánek, T., Hradecký, J., Stoffel, M., 2013. Regional, dendrogeomorphic chronologies of debris flows for the Crimean Mountains (Ukraine): frequency and impacts of tree age on results. *Earth Surf. Process. Land.* (in press).
- Solomina, O., Pavlova, I., Curtis, A., Jacoby, G., Panomareva, V., Pevzner, M., 2008. Constraining recent Shiveluch volcano eruptions (Kamchatka, Russia) by means of dendrochronology. *Nat. Hazards Earth Syst. Sci.* 8, 1083–1097.
- Stahle, D., Villanueva, J., Cleaveland, M.K., Therrell, M.D., Paull, G.J., Burns, B.T., Salinas, W., Suzan, H., Fule, P., 2000. Recent tree-rings research in Mexico. *Dendrogeomorfología en América Latina*. F.A. Roig (comp); EDIUV, Mendoza, Argentina, 285–306.
- Stoffel, M., Bollschweiler, M., 2008. Tree-ring analysis in natural hazards research—an overview. *Nat. Hazards Earth Syst. Sci.* 8, 187–202.
- Stoffel, M., Corona, C., 2013. Dendroecological dating of (hydro-) geomorphic disturbance in trees. *Tree-Ring Res.* (in press).
- Stoffel, M., Perret, S., 2006. Reconstructing past rockfall activity with tree rings: some methodological considerations. *Dendrochronologia* 24 (1), 1–15.
- Stoffel, M., Wilford, D.J., 2012. Hydrogeomorphic processes and vegetation: disturbance, process histories, dependencies and interactions. *Earth Surf. Process. Land.* 37, 9–22.
- Stoffel, M., Lièvre, I., Monbaron, M., Perret, S., 2005. Seasonal timing of rockfall activity on forested slope at Täschgüfer (Swiss Alps)—a dendrogeomorphological approach. *Z. Geomorphol.* 49, 89–106.
- Stoffel, M., Conus, D., Grichting, M.A., Lièvre, I., Maître, G., 2008. Unraveling the patterns of late Holocene debris-flow activity on a cone in the central Swiss Alps: chronology, environment and implications for the future. *Glob. Planet. Chang.* 60, 222–234.
- Stoffel, M., Bollschweiler, M., Butler, D., y Luckman, B. (Eds.), 2010. *Tree Rings and Natural Hazards: A State-of-the-Art*. Springer, Berlin, Heidelberg, New York (505 pp.).
- Stoffel, M., Bollschweiler, M., Vázquez-Selem, L., Franco-Ramos, O., Palacios, D., 2011. Dendrogeomorphic dating of rockfall on low-latitude, high-elevation slopes: Rodadero, Iztaccíhuatl volcano, México. *Earth Surf. Process. Land.* 36, 1209–1217.
- Stoffel, M., Casteller, A., Luckman, B.H., Villalba, R., 2012. Spatiotemporal analysis of channel wall erosion in ephemeral torrents using tree roots—an example from the Patagonian Andes. *Geology* 40 (3), 247–250.
- Stoffel, M., Rice, S., Turowski, J.M., 2013. Process geomorphology and ecosystems: disturbance regimes and interactions. *Geomorphology* 202, 1–4.
- Villanueva Díaz, J., Cerano Paredes, J., Stahle, D.W., Constante García, V., Vázquez Selem, L., Estrada Avalos, J., Benavides Solorio, J., 2010. Árboles longevos de México. *Revista Mexicana de Ciencias Forestales*, vol. 1, Núm. 2, pp. 7–29.
- Yanosky, T.M., Jarrett, R.D., 2002. Dendrochronologic evidence for the frequency and magnitude of paleofloods. In: House, P.K., Webb, R.H., Baker, V.R., Levish, D.R. (Eds.), *Ancient Floods, Modern Hazards: Principles and Applications of Paleoflood Hydrology*, 5. American Geophysical Union, Water Science and Application Series, pp. 77–89.
- Zobin, V.M., Santiago-Jiménez, H., Ramírez-Ruiz, J.J., Reyes-Dávila, G.A., Bretón-González, M., Navarro-Ochoa, C., 2007. Quantification of volcanic explosion from tilt records: Volcán de Colima, México. *J. Volcanol. Geotherm. Res.* 166, 117–124.
- Zobin, V.M., Plascencia, I., Reyes, G., Navarro, C., 2009. The characteristics of seismic signals produced by lahars and pyroclastic flows: Volcán de Colima, México. *J. Volcanol. Geotherm. Res.* 179, 157–167.